In-House Design, Manufacturing, and Testing of a 2.856 GHz Combline Microwave Cavity Filter for the Low-Level RF Systems of Linear Particle Accelerators

Giacomo Giannetti[1], Marco Bellaveglia[2], Alessandro Gallo[2], Stefano Maddio[1], Andrea Mostacci[3], Luca Piersanti[2], Beatrice Serenellini[2], Stefano Selleri[1], Simone Tocci[2]

[1]Department of Information Engineering, University of Florence, Via di Santa Marta 3, I-50139, Florence (FI), Italy
[2]Laboratori Nazionali di Frascati, Istituto Nazionale di Fisica Nucleare, Via Enrico Fermi 54, I-00044, Frascati (RM), Italy
[3]Department of Basic and Applied Sciences for Engineering, La Sapienza University, Via Antonio Scarpa 14, I-00161, Rome (RM), Italy

Corresponding author: G. Giannetti (e-mail: giacomo.giannetti@unifi.it)

ABSTRACT A combline microwave cavity filter has been developed to generate the 2.856 GHz radio frequency (RF) tone to be used as the master reference of SPARC_LAB electron linac facility at the Frascati National Laboratories of the National Institute for Nuclear Physics (LNF-INFN). The filter must select the 36th harmonic from a frequency comb with a repetition frequency of 79.33 MHz and reject the other harmonics. The comb is generated by the electric conversion of the laser pulse train from the oscillator of the photocathode laser. Since a filter for this very specific application is off-the-shelf, it was designed, manufactured, and tested in-house at LNF-INFN. The measured insertion loss at the center frequency is 2.2 dB, the bandwidth is 30 MHz (percentage fractional bandwidth is 1.1 %). This narrow bandwidth is required to ensure effective rejection (insertion loss $>$ 65 dB) of adjacent harmonics in the frequency comb, specifically at frequencies of 2.77633 GHz and 2.93533 GHz. The purpose of filtering is to ensure that the tone, distributed in the low-level RF system, remains clean and can be used to synchronize the most crucial machine subsystems, such as RF power units, accelerating cavities, diagnostic systems, and lasers.

INDEX TERMS combline cavity filters, low-level RF systems, microwave filters, particle accelerators

I. INTRODUCTION

MICROWAVE cavity filters play a crucial role in low-level radio frequency (LLRF) systems of linear particle accelerators [1]–[3]. These filters are commonly used in various subsystems, such as down-converter stages, to eliminate unwanted intermodulation products that may arise from mixers. This is particularly important when there is a separation between the RF and local oscillator frequencies in the range of a few tens of megahertz. Additionally, microwave cavity filters are employed in reference generation stages to select the desired harmonic from a frequency comb, as well as in the LLRF systems to remove any spurious frequencies prior to the final amplification of the drive signal.

In the SPARC_LAB facility [4] at LNF-INFN, microwave cavity filters are currently used to select the 2.856 GHz tone to be distributed as the facility master reference from a frequency comb generated by a fast photodiode (EOT 3500F), placed at the output of the photocathode laser oscillator cavity. This cavity produces an ultrashort laser pulse train (power 1 W, pulse length 10 fs, wavelength 800 nm), whose repetition rate (79.33 MHz) is a subharmonic of the SPARC_ LAB RF reference. In frequency domain, the pulse train is represented by a comb of harmonics, multiples of the repetition rate frequency. Thus, the facility RF reference, that is, the 36th harmonic of the comb, can be extracted from the pulse train using an optical to electrical transducer (the photodiode) and a selective filter.

For common applications, these filters are available on the market from several industrial manufacturers with a wide range of prices and quality. However, for a specific application as the one outlined, these filters can be expensive, come sometimes with fixed frequencies or bandwidth, and the lead time can be several months because custom off-the-shelf products are required. To have complete control over microwave specifications and manufacturing time, an inexpensive combline microwave filter centered at 2.856 GHz has been designed, manufactured, and tested at LNF-INFN. Not least, the design of microwave filters requires specific knowledge that is often outside of the skills for RF technicians and engineers working on particle accelerators. The

second significant contribution of this work is then to make RF practitioners in particle accelerators familiar with the interesting yet exclusive world of microwave filters.

II. DESIGN

A. SPECIFICATIONS AND RESPONSE SYNTHESIS

The filter specifications are as follows. The center frequency is $f_0 = 2.856\,\text{GHz}$ and the bandwidth $\text{BW} = 30\,\text{MHz}$ (the percentage fractional bandwidth is $\text{FBW}(\%) = 100 \cdot \text{BW}/f_0 = 1.1\,\%$). Return loss must be at least 20 dB in the passband. The unwanted signals are at $f_0 \pm \Delta$, $\Delta = 79.33\,\text{MHz}$, that is, 2.77633 GHz and 2.93533 GHz, and the insertion loss must be greater than 65 dB at these frequencies. To meet the specifications, a Chebyshev response with a passband ripple of 0.01 dB, corresponding to a minimum return loss of 26.4 dB, is considered. Regarding the filter order, $N = 5$ is the minimum value allowing to satisfy the desired attenuation at $f_0 \pm \Delta$. Higher values would also meet the specifications, but at the cost of higher complexity and loss. The lossy synthesized response is shown in Fig. 6.

The $(N+2) \times (N+2)$ coupling matrix $\mathbf{M} = [m_{ij}]$ [5] for the synthesized response is

$$\mathbf{M} = \begin{bmatrix} 0 & 1.150 & 0 & 0 & 0 & 0 & 0 \\ 1.150 & 0 & 1.007 & 0 & 0 & 0 & 0 \\ 0 & 1.007 & 0 & 0.697 & 0 & 0 & 0 \\ 0 & 0 & 0.697 & 0 & 0.697 & 0 & 0 \\ 0 & 0 & 0 & 0.697 & 0 & 1.007 & 0 \\ 0 & 0 & 0 & 0 & 1.007 & 0 & 1.150 \\ 0 & 0 & 0 & 0 & 0 & 1.150 & 0 \end{bmatrix} \tag{1}$$

where m_{ij} are the normalized coupling coefficients. Note that a) only adjacent resonators are coupled, since only the terms $m_{i,i+1}$ and $m_{i+1,i}$, $i = 1, \ldots, 5$ are not zero, and that b) the input (output) port is connected to the first (last) resonator only, since only the term $m_{0,1}$ ($m_{6,7}$) is not zero. These two facts are graphically explained by the filter topology depicted in Fig. 1.

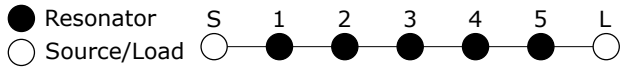

FIGURE 1: Topology of the filter.

B. FILTER TECHNOLOGY AND DIMENSIONS

To translate the synthesized response into a physical description of the filter, it is necessary to denormalize the coupling matrix and to choose a filter technology.

Denormalizing the coupling matrix, the coupling coefficients are given by

$$K_{i,i+1} = m_{i,i+1}\text{FBW}, \quad i = 1, \ldots, N-1 \tag{2}$$

and the external quality factors of input and output ports by

$$Q_E^{IN} = \frac{1}{m_{0,1}^2 \text{FBW}} \qquad Q_E^{OUT} = \frac{1}{m_{5,6}^2 \text{FBW}}. \tag{3}$$

From (2), (3), and the coupling matrix (1), it turns out that $K_{1,2} = K_{4,5} = 0.0106$, $K_{2,3} = K_{3,4} = 0.0073$, and $Q_E^{IN} = Q_E^{OUT} = 72.0$.

For the realization, the combline cavity filter technology is chosen. A panoramic view of the filter model in the CST simulator [6] and its technical drawing are displayed in Fig. 2. The filter is composed of N coaxial resonators that are grounded at one extremity and capacitively loaded at the other. They must resonate at the filter center frequency. To have a fine tuning of the resonance frequency, tuning screws are added at the free end of the coaxial resonators and penetrate into the latter. The first and last resonators are fed by tap-inductive coupling. This is achieved, on one hand, by soldering copper pins to the SMA connectors and, on the other hand, by putting the copper pins in galvanic contact with the end resonators. The tap coupling must realize the desired external quality factor from (3). Instead, adjacent resonators must be characterized by a coupling coefficient equal to (2). For a fine-tuning of the coupling between adjacent resonators, coupling screws are added midway two adjacent resonators. For further details on this filter technology, the reader is referred to [5], [7]–[10].

With reference to Fig. 2.b, the height of the coaxial resonators is $L = \lambda/8 = 13.1\,\text{mm}$ [10], with $\lambda = 105\,\text{mm}$ the free space wavelength at f_0. Shorter $\lambda/8$ resonators are preferred over longer $\lambda/4$ ones [11] for compactness. The diameter of both the tuning and coupling screws is $D = 3\,\text{mm}$ and it is selected to use standard M3 screws as tuning element instead of the more expensive commercial tuners. From the screw diameter, the inner diameter of the coaxial resonators is set to $D_i = 5.5\,\text{mm}$ to have about 1 mm-margin between the tuning screws and the coaxial resonators. Consequently, the outer diameter of the coaxial resonators is $D_o = 7.5\,\text{mm}$ to have the resonator walls of 1 mm. The distance from the free ends of the resonators to the lid is set to $G = 4\,\text{mm}$ as in [10],

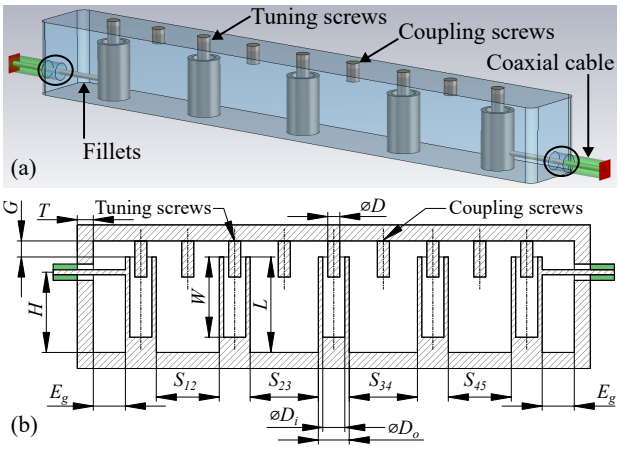

FIGURE 2: Filter: (a) CST model; (b) technical drawing. In (a), the circles next to the input and output ports are positioned to highlight the cavity thickness. In (b), the cavity width and the radius of the fillets are b and r, respectively.

the resonators are milled to a depth equal to $W = 11.1\,\text{mm}$ to host the tuning screws.

To find the other geometrical values, parametric analyses are performed. In Fig. 3.a, the unloaded quality factor versus the width of the cavity is shown. The enclosure, the resonator, and the tuning screw are made of brass here and in the following (conductivity: $2.74 \cdot 10^7$ S/m). From Fig. 3.a, the width of the cavity $b = 16\,\text{mm}$, corresponding to a simulated unloaded quality factor of $Q_u = 2.1 \cdot 10^3$, is selected as a compromise between compactness and unloaded quality factor. For the coupling between adjacent resonators, a parametric sweep for the distance between adjacent resonators is performed and the results are drawn in Fig. 3.b. For this study, a coupling screw with a $5\,\text{mm}$-penetration is added. The distances between resonators $s_{12} = s_{45} = 19.0\,\text{mm}$, $s_{23} = s_{34} = 21.2\,\text{mm}$ realize the desired values of the coupling coefficients (2). Eventually, Fig. 3.c reports the external quality factor versus the height of the coaxial hole H, being the distance between the end resonators and the cavity $E_g = 12\,\text{mm}$. A value $H = 3.8\,\text{mm}$ realizes the target value of Q_E (3). For this study regarding the values of E_g and H, the reader is also referred to [7], [12].

The radius of the fillets is $r = 2\,\text{mm}$ since a cutter tip with a 4 -mm diameter is used for manufacturing and the thickness of the cavity is $T = 4\,\text{mm}$ so that M2 screws can be used to fasten the lid.

III. REALIZATION AND MEASUREMENTS

The realized filter is made of brass and is shown in Fig. 4. A 5-axis computerized numerical control machine from C.B.Ferrari [13] has been used. Its maximum resolution is $1\,\mu\text{m}$ while its maximum precision is $10\,\mu\text{m}$. The cavity is split into two parts: the lid and the main body. The resonators are integrated into the main body, eliminating the need to secure them with screws. M3 brass screws are used as tuning and coupling screws, while M3 lock nuts are used for finer control in the tuning stage. The cover is fixed to the main body with 18 M2 screws to ensure RF contact and avoid RF leakage. The number of screws used to seal the lid is a compromise between assembly time and potential power leakage. The type of SMA connectors is panel mount plug with solder cup. The lid and the main body are the only two pieces that must be manufactured ad hoc (custom off-the-shelf), while the others are commercially available.

A. EXTERNAL QUALITY FACTOR

Due to manufacturing limitations, the height H of the coaxial hole is higher than that foreseen ($11.1\,\text{mm}$ instead of $3.8\,\text{mm}$). Then, to obtain the target value for the external quality factors of the input and output ports (3), the copper pins are bent, as visible in Fig. 4.a. To adjust the bending, we rely on the parametric analysis for the external quality factor versus the height of the touch point h in Fig. 3.d and on the measured group delay. Indeed, in case of over-coupling [14], the expression relating the external quality factor to the group

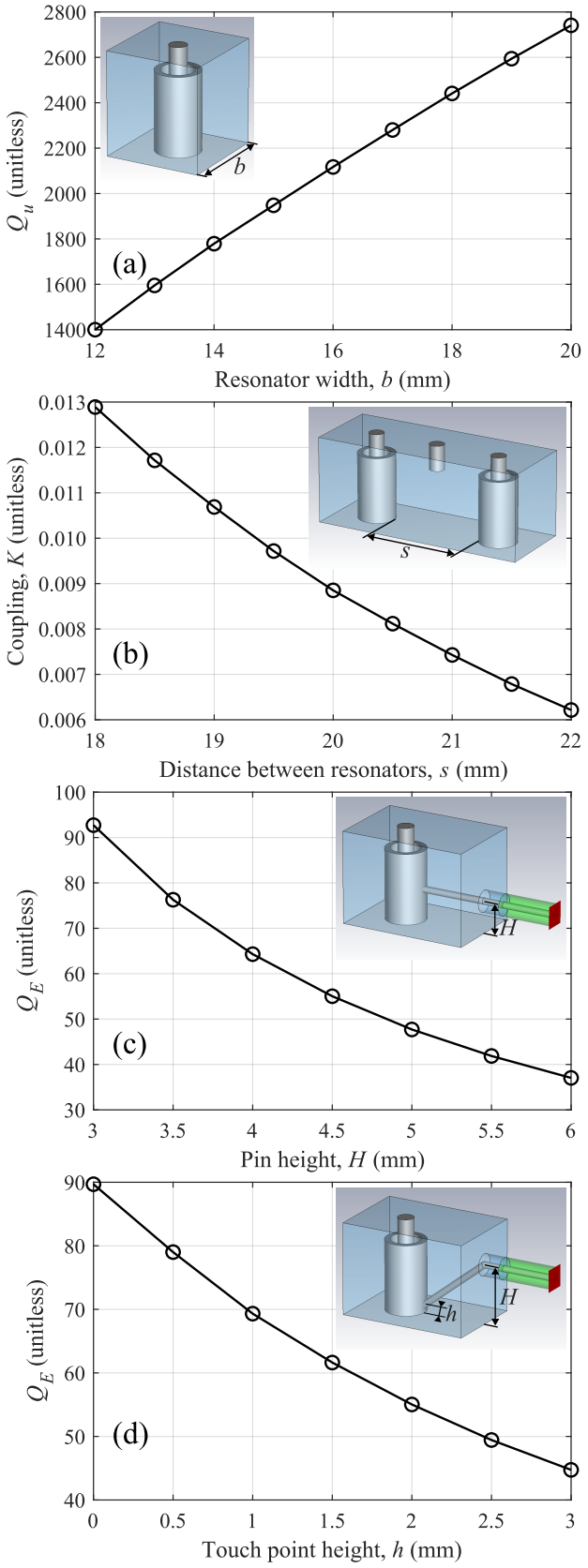

FIGURE 3: Parametric analyses: (a) unloaded quality factor; (b) coupling coefficient; (c) and (d) external quality factors in case of straight and bent pin, respectively.

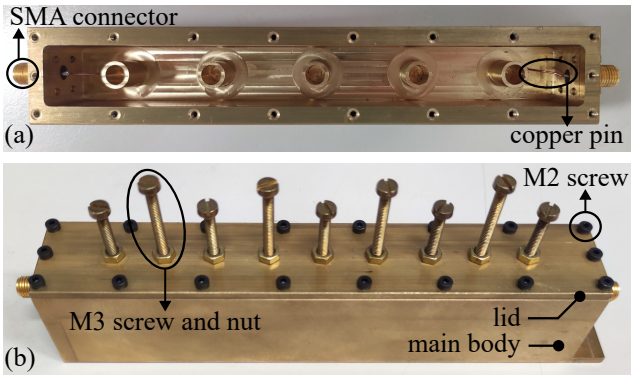

FIGURE 4: Pictures of the filter prototype with annotations: (a) uncovered; (b) assembled.

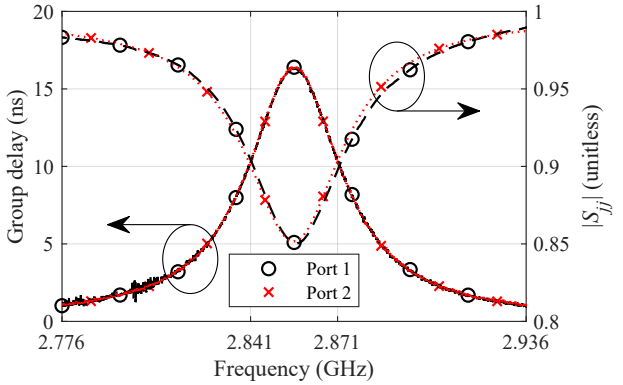

FIGURE 5: Group delay and reflection coefficient at the two ports with the two end resonators tuned to resonance and the others short-circuited.

delay at port j, $\Gamma_{d,j}$, is [15]

$$\Gamma_{d,j} = \frac{2}{\pi f_0} \frac{Q_E}{1 - \left(\frac{Q_E}{Q_u}\right)^2} \tag{4}$$

$$\frac{Q_E}{Q_u} = \frac{1 - |S_{jj}(f_0)|}{1 + |S_{jj}(f_0)|} \tag{5}$$

being Q_u the unloaded quality factor and S_{jj} the reflection coefficient at port j. In (4) and (5), Q_E and Q_u should be specified for the input and output ports. However, this distinction is not made for simplicity. Inverting (4) and using (5), the external quality factor can be derived from the measured group delay and reflection coefficient.

In Fig. 5, the measured group delay and reflection coefficient for both ports are shown, under the condition described in [7], [15] (all resonators, except the one being measured, are short-circuited by screwing the tuning screws to stop; the coupling screws are extracted). At center frequency, the group delay measured for both ports is 16.4 ns and $|S_{jj}(f_0)|$ is 0.85, corresponding to an external quality factor realized of 73.1 from (4) and (5), just 1.5 % greater than the desired target value (3). Throughout the paper, the measurement instrument is the VNA N5242A from Agilent Technologies, calibrated with 2-port SOLT calibration [16].

B. FILTER TUNING AND RESPONSE

After the adjustment of the tap coupling, the filter is tuned by adjusting the penetration of the screws inside the cavity. For this scope, the CST software [6] has been used, as it offers a dedicated package for tuning based on the coupling matrix. This tool specifically computes the coupling matrix realized from the measured scattering parameters to indicate the direction in which the screws should be screwed.

The measured tuned response is shown in Fig. 6. The insertion loss at the center frequency is 2.2 dB and the return loss is greater than 24 dB in the bandwidth of interest. The rejection relative to the center frequency of the unwanted frequencies 2.77633 GHz and 2.93533 GHz is 66.1 dBc and 66.9 dBc, respectively. The filter then fulfills specifications.

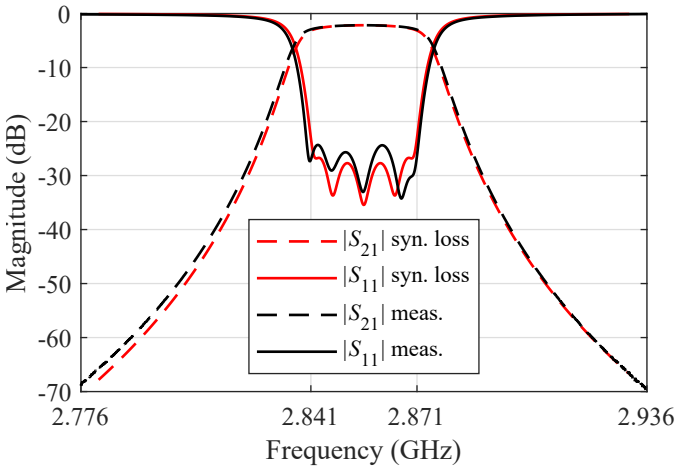

FIGURE 6: Magnitude of the scattering parameters. In the legend, the abbreviations syn. and meas. represent the synthesized response and the measured response, respectively. The average unloaded quality factor for the lossy synthesized response is $1.09 \cdot 10^3$.

In Fig. 6, the lossy synthesized response is also drawn for comparison. This is found by equating the insertion losses at the center frequency from the measurements and the lossy prototype passband response. The latter is obtained by performing a lossy lowpass-to-bandpass transformation [15]. This transformation has the unloaded quality factor as the free parameter and, therefore, it is possible to estimate the average unloaded quality factor as $\bar{Q}_u = 1.09 \cdot 10^3$, where the bar remarks the average. The measured $\bar{Q}_u$ is within the range $200 - 3000$ for coaxial resonators [17], but one thousand less than the simulated value in Fig. 3.a. In general, excellent agreement can be observed between the lossy synthesized response and the measurements in Fig. 6.

At SPARC_LAB, S-band and C-band accelerating structures coexist. This may lead to interference between components, thus compromising the proper working of the LLRF system. A broadband characterization of the filter is then

TABLE 1: Performance comparison. Ref.=reference, f_0 center frequency, FBW=fractional bandwidth, Vol.=volume, $\text{FoM}_1 = \text{Vol.}/N$, $\text{FoM}_2 = \bar{Q}_u/\text{FoM}_1$; TW=this work; RL=return loss; IL=insertion loss; sim.=simulated.

Ref.	f_0 (GHz)	N	FBW (%)	RL (dB)	IL (dB)	Vol. $(\cdot 10^2\lambda^3)$	$Q_u(\cdot 10^3)$	$\text{FoM}_1(\cdot 10^2\lambda^3)$	FoM_2 $(\cdot 10^{-4}\lambda^{-3})$
[1]	11.822	7	0.5	>11	12	–	–	–	–
[10]	2.8	5	9	>13	0.56	1.6	–	0.32	–
[9]	1.575	5	2.0	>19	1.72	0.9	0.8	0.17	46.6
[11]	3.95	8	12.7	>20	0.7-0.9	27.1	7 (sim.)	3.4	20.7
[21]	2.4	9	10.8	25	1.39	–	–	–	–
TW	2.856	5	1.1	>24	2.2	3.4	1.09	0.7	16.2

needed. This is provided in Fig. 7, which shows the wideband response for $|S_{21}|$ from 2 GHz to 12 GHz. The filter response is spurious-free up to 8 GHz, the first spurious window occurring at around $3f_0$. This means that the C-band and, in particular, the $2f_0 = 5.712$ GHz signal, used in C-band accelerating cavities, are properly suppressed.

A power handling analysis is carried out in case of high-power operation. In operation, the filter is filled with dry air at a temperature of 293.15 K and a pressure of 1 bar. Due to this pressure, the breakdown may occur only due to corona discharge, not multipaction [18]. According to the tool Spark3D [19], the power threshold is 174.4 W, 76.0 W, and 74.8 W at f_0, 2.839 GHz, and 2.875 GHz, respectively. The last two frequencies are characterized by a maximum of the group delay and, consequently, by a maximum of the energy stored inside the cavity [18]. The conservative value for the maximum input power is then 74.8 W.

The designed filter is compared with other examples of cavity filters in Table 1. The insertion loss of the presented filter is the second highest. This is because the insertion loss is inversely proportional to the $\bar{Q}_u$ and the FBW [20], that for the proposed filter is the second lowest. Insertion loss may then be decreased by increasing the $\bar{Q}_u$ (the FBW is fixed as per specification). The $\bar{Q}_u$ can be increased by varying the shapes of the resonators and lid or by plating the filter with a highly conductive material. The volume per resonator is low even if not one of the best. Interestingly, the proposed filter outperforms the one designed so far for LLRF systems [1].

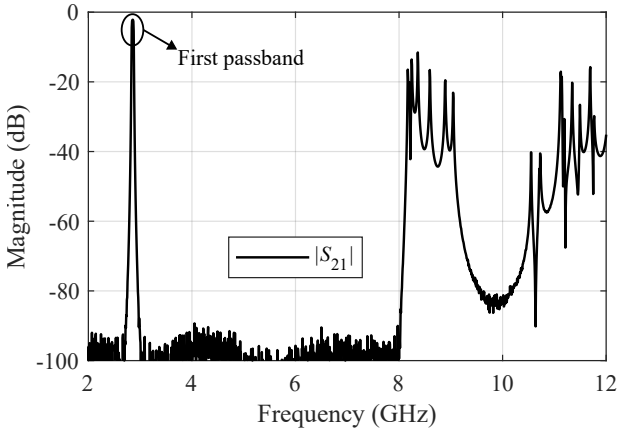

FIGURE 7: Wideband measured response for $|S_{21}|$.

IV. CONCLUSION

The manuscript presents a combline microwave cavity filter to be used in LLRF systems for linear particle accelerators. The design is suitable for in-house manufacturing at LNF-INFN and presents an excellent response in terms of insertion loss at the center frequency, bandwidth, and selectivity (the rejection of unwanted harmonics is greater than 65 dB).

The next step is to design and build in-house filters for the C and X bands, that are also of great interest for LLRF applications at LNF-INFN. In addition, future studies should aim to design reflectionless filters [22], [23], so to avoid that undesired signals are reflected back and circulate in the LLRF systems.

DATA AVAILABILITY STATEMENT

The CST model of the filter and the data of the measured and synthesized responses in Fig. 5-7 are available at DOI 10.5281/zenodo.10670431.

DECLARATION OF GENERATIVE AI AND AI-ASSISTED TECHNOLOGIES IN THE WRITING PROCESS

The tool writefull [24], which is based on artificial intelligence, has been used to help to formulate the text in better English. After using this tool, the authors reviewed and edited the content as needed and take full responsibility for the content of the publication. Artificial intelligence has not been used to develop the content presented in the paper.

REFERENCES

[1] A. V. Edwards, M. Boronat Arevalo, N. Catalán Lasheras, A. C. Dexter, and G. McMonagle, "Commissioning of a new X-band, low-noise LLRF system," in Proc. IPAC, Campinas, SP, Brazil, 2021, pp. 2683–2686. DOI: 10.18429/JACoW-IPAC2021-WEPAB038.

[2] L. Piersanti et al., "Design of an X-band LLRF system for TEX test facility at LNF-INFN," in Proc. IPAC, Campinas, SP, Brazil, 2021, pp. 3371–3374. DOI: 10.18429/JACoW-IPAC2021-WEPAB301.

[3] L. Piersanti et al., "Commissioning and first results of an X-band LLRF system for TEX test facility at LNF-INFN," in Proc. IPAC, Bangkok, BKK, Thailand, 2022, p. 12075. DOI: 10.1088/1742-6596/2420/1/012075.

[4] M. Ferrario et al., "SPARC-LAB present and future," Nuclear Instruments and Methods in Physics Research, Section B: Beam Interactions with Materials and Atoms, vol. 309, pp. 183–188, 2013, DOI: 10.1016/j.nimb.2013.03.049.

[5] R. J. Cameron, C. M. Kudsia, and R. R. Mansour, Microwave Filters for Communication Systems, 2nd ed. Hoboken, NJ, USA: Wiley, 2018. DOI: 10.1002/9781119292371.

[6] Dassault Systèmes, "CST Studio Suite," 2025. [Online]. Available: https://www.3ds.com/products-services/simulia/products/cst-studio-suite/

[7] E. Boni, G. Giannetti, S. Maddio, and G. Pelosi, "Fast and efficient systematic procedure for and flexibility on the end coupling design in microwave filters," in Proc. KH2023, Miltenberg, BY, Germany, 2023. [Online]. Available: https://ieeexplore.ieee.org/document/10296826

[8] E. Boni, G. Giannetti, S. Maddio, and G. Pelosi, “Capacitive end-couplings in combline microwave cavity filters with probe parallel to resonators’ axes: comparison and design guidelines,” in Proc. KH2023, Miltenberg, BY, Germany, 2023. [Online]. Available: https://ieeexplore.ieee.org/document/10296707

[9] E. Boni, G. Giannetti, S. Maddio, and G. Pelosi, “Comparison of inductive and capacitive end couplings in the design of a combline microwave cavity filter for the E1 Galileo band,” Advances in Radio Science, vol. 22, pp. 1–8, 2024, DOI: 10.5194/ars-22-1-2024.

[10] M. S. Anwar and H. R. Dhanyal, “Design of S-band combline coaxial cavity bandpass filter,” in Proc. IBCAST, Islamabad, IS, Pakistan, 2018, pp. 866–869. DOI: 10.1109/IBCAST.2018.8312328.

[11] Y. P. Yu and Y. F. Li, “Design of a small size C-band cavity bandpass filter,” Microwave and Optical Technology Letters, vol. 64, no. 9, pp. 1507–1512, 2022, DOI: 10.1002/mop.33307.

[12] E. Boni, G. Giannetti, S. Maddio, and G. Pelosi, “An equation-based method for the design of end couplings in combline microwave cavity filters,” in Proc. IEEE AP-S, Portland, OR, USA, 2023, pp. 1473–1474. DOI: 10.1109/USNC-URSI52151.2023.10237496.

[13] C.B.Ferrari s.r.l., "C.B.Ferrari," 2025. [Online]. Available: https://www.cbferrari.com/en/

[14] D. M. Pozar, Microwave Engineering, 4th ed. New York, NY, USA: Wiley, 2011.

[15] J. B. Ness, “A unified approach to the design, measurement, and tuning of coupled-resonator filters,” IEEE Transactions on Microwave Theory and Techniques, vol. 46, no. 4, pp. 343–351, 1998, DOI: 10.1109/22.664135.

[16] A. Rumiantsev and N. Ridler, “VNA calibration,” IEEE Microwave Magazine, vol. 9, no. 3, pp. 86–99, 2008, DOI: 10.1109/MMM.2008.919925.

[17] R. Mansour, “High-Q tunable dielectric resonator filters,” IEEE Microwave Magazine, vol. 10, no. 6, pp. 84–98, 2009, DOI: 10.1109/MMM.2009.933591.

[18] M. Yu, “Power-handling capability for RF filters,” IEEE Microwave Magazine, vol. 8, no. 5, pp. 88–97, 2007, DOI: 10.1109/MMM.2007.904712.

[19] Dassault Systèmes, "Spark3D," 2025. [Online]. Available: https://www.3ds.com/products/simulia/spark3d

[20] D. G. Swanson, “Narrow-band microwave filter design,” IEEE Microwave Magazine, vol. 8, no. 5, pp. 105–114, 2007, DOI: 10.1109/MMM.2007.904724.

[21] A. Agarwal, R. Sharma, V. Srivani, and M. T. Wara, “Design of wide bandwidth filter at S-band for spacecraft testing applications,” in Proc. SPACE, Bangalore, KA, India, 2024, pp. 986–989. DOI: 10.1109/SPACE63117.2024.10668228.

[22] D. Psychogiou and R. Gomez-Garcia, “Reflectionless adaptive RF filters: bandpass, bandstop, and cascade designs,” IEEE Transactions on Microwave Theory and Techniques, vol. 65, no. 11, pp. 4593–4605, 2017, DOI: 10.1109/TMTT.2017.2734086.

[23] R. Gomez-Garcia, D. Psychogiou, J. M. Munoz-Ferreras, and L. Yang, “Avoiding RF isolators: reflectionless microwave bandpass filtering components for advanced RF front ends,” IEEE Microwave Magazine, vol. 21, no. 12, pp. 68–86, 2020, DOI: 10.1109/MMM.2020.3023222.

[24] Writefull, "Writefull," 2025. [Online]. Available: https://www.writefull.com/